International Journal of Mechanical, Industrial and Aerospace Sciences
ISSN: 2517-9950
Vol:6, No:8, 2012

Numerical Study of Natural Convection Effects in Latent Heat Storage using Aluminum Fins and Spiral Fillers

Lippong Tan, Yuenting Kwok, Ahbijit Date, Aliakbar Akbarzadeh

***Abstract*—**A numerical investigation has carried out to understand the melting characteristics of phase change material (PCM) in a fin type latent heat storage with the addition of embedded aluminum spiral fillers. It is known that melting performance of PCM can be significantly improved by increasing the number of embedded metallic fins in the latent heat storage system but to certain values where only lead to small improvement in heat transfer rate. Hence, adding aluminum spiral fillers within the fin gap can be an option to improve heat transfer internally. This paper presents extensive computational visualizations on the PCM melting patterns of the proposed fin-spiral fillers configuration. The aim of this investigation is to understand the PCM's melting behaviors by observing the natural convection currents movement and melting fronts formation. Fluent 6.3 simulation software was utilized in producing two-dimensional visualizations of melting fractions, temperature distributions and flow fields to illustrate the melting process internally. The results show that adding aluminum spiral fillers in Fin type latent heat storage can promoted small but more active natural convection currents and improve melting of PCM.

***Keywords*—**Phase change material, thermal enhancement, aluminum spiral fillers, fins

I. Introduction

THERMAL storage systems play important roles in energy conservation for environmental and civil engineering. Designing an effective thermal storage system is able to reduce the mismatch between supply and demand of energy. Solar heating system is one of the examples used in civil engineering where sensible storage systems are utilized for storing heat energy dissipated by the sun and reuse it for thermal conditioning such as air and water supply in buildings. Latent heat heat storage (LHS) has higher heat storage density due to the present of latent heat of fusion of which material undergoing phase change. For instance, typical rock-based sensible heat storage requires seven times of storage mass compared to paraffin 116 wax (PCM) for storing the same amount of heat energy [1-2]. It also possesses nearly isothermal operation which allows the desired temperature to maintain for a longer period.

L. P. Tan is with the Energy Conservation and Renewable Energy Group, RMIT University, Melbourne, Australia (e-mail: lippong.tan@rmit.edu.au).

Y. T. Kwok is with the Energy Conservation and Renewable Energy Group, RMIT University, Melbourne, Australia (e-mail: s3187853@student.rmit.edu.au).

A. Date is with the Energy Conservation and Renewable Energy Group, RMIT University, Melbourne, Australia (e-mail: abhijit.date@rmit.edu.au).

A. Akbarzadeh is with the Energy Conservation and Renewable Energy Group, RMIT University, Melbourne, Australia (e-mail: aliakbar.akarzadeh@rmit.edu.au).

This technology is further exploited in electronics cooling where PCMs are used for regulating the operating temperature of the electronic devices [3].

Despite the fact that LHS serves as high thermal storage density, sensible heat method is still the preferred method for thermal storage system design. The main issue on using latent heat method lies on the poor thermal conductivity of the PCM which limits the rate of heat absorbing and releasing. For example, commercial paraffin waxes are cheap and delivered acceptably high heat storage density (~200 kJ) with wide range of melting temperatures. They are also chemically stable, high thermal cyclic and no phase segregation which make them ideal PCM in the thermal storage system. However, the low thermal conductivity (~0.2W/m K) has greatly limited their potentials and applications. In spite of inorganic salt hydrates have higher thermal conductivity (~0.5W/m K) and energy density (~450KJ/kg), phase segregation and super-cooling are unfavorable in thermal storage design. To embark on economical and feasible storage system, simple thermal enhancement method must develop to improve the heat transfer performance. If not, this technology will still remain as unsuccessful for large scale applications.

Published literatures [4-5] have reviewed on various thermal enhancement methods for improving the heat transfer and melting performance of LHS systems. In summary, these approaches are: using extended surface (fins), employing multiple PCM's method, metal matrix, metallic fillers and micro-encapsulation. In this present investigation, thermal enhancement method using fins will be discussed in detailed.

Using metallic fins is one of the simple and effective approaches for improving the melting rate of PCM in the thermal storage. However, the increasing number of internal fins will not linearly contribute to a sharp increase in the overall heat transfer coefficient. This is because natural convection heat transfer effect is diminished within the smaller fin gap volume. Gharebagi and Sezai [6] have investigated the performance of rectangular PCM device with horizontal fins added to heated vertical walls. They found out that with the increasing of fins only leaded to a marginal increase in heat transfer rate. Thus, concluded that increasing number of fin will hamper the effect of natural convection within the system and melting would become a conduction-dominated process. Lamberg et al. [7] has conducted an experimental and numerical study on melting performance of PCM in a rectangular enclosure, with and without natural convection effect. The results showed that PCM took double the time to reach the maximum temperature when natural convection

effect was ignored. Jellouli et al. [8] also did similar experiment on melting of PCM in rectangular enclosure with heating at the bottom. The isotherms obtained were horizontal at the early stage and became accentuated at the latter stage. Based on this phenomenon, he concluded that conduction dominated melting process at the early stage and gradually shifted to natural convection effect during melting test.

The objective of this work is to investigate numerically on the melting behaviors of adding aluminum spiral fillers into fin type rectangular LHS. As mentioned in the literature that increasing number of fins would not experience great improvement in melting, the authors aim to improve the heat transfer performance by optimizing both conduction and natural convection heat transfer effects during melting by adding aluminum fillers. In this paper, extensive numerical simulations have been carried out where simulated visualizations were developed for observing the PCM melting effects and patterns. Melt fractions, temperature distributions and flow fields at various heating durations are visually presented.

II. Numerical Analysis

In this section, two different LHS (slab) configurations show in Fig. 1 have experimentally and numerically investigated. Commercial simulation software (Fluent 6.3) is used to solve the conservation equations for mass, momentum and energy. A physical model of the system and the computational procedure are presented in detail in this section.

A. Experimental set-up

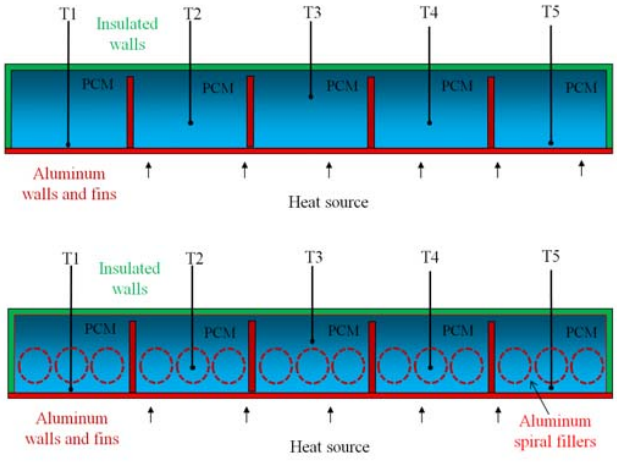

Fig. 1 Experimental slabs filled with PCM: Fin-type (Top), Fin-spiral fillers (Bottom)

The main components in the experiment are paraffin wax as PCM and two aluminum rectangular slabs with physical dimensions of 300mm (length) x 300mm (width) x 25mm (depth). Four aluminum fins are installed in both rectangular slab and Fins-Spiral slab configuration is added with twelve aluminum spiral fillers at diameter of 12mm. Commercial paraffin wax is used as PCM in the experimental and numerical investigation. In order to understand the specific heat capacity variation over temperature of the PCM during melting, samples of paraffin wax (~10mg) were sent to RMIT chemical department for differential scanning calorimetry (DSC). The DSC scanning results in Fig. 2 shows that the peak melting temperature is 47^{o}C with latent heat of ~140kJ/kg. The summarized thermo-physical properties are detailed in Tab. 1.

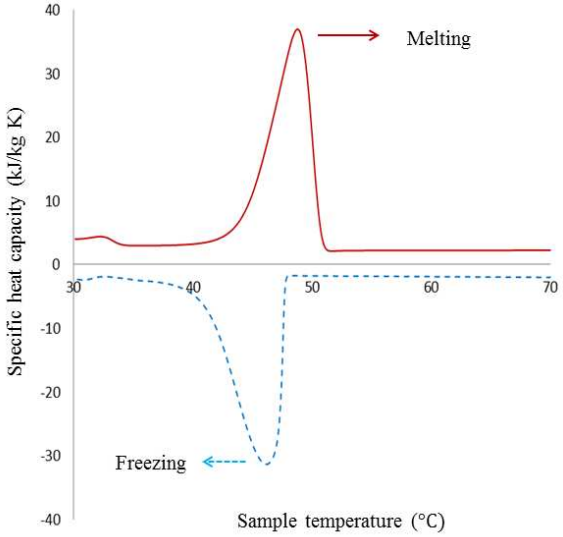

Fig. 2 DSC results for paraffin wax

TABLE I
THERMO-PHYSICAL PROPERTIES OF TESTED PARAFFIN WAX

Parameters	*Values*
Density [kg/m^3]	880 (solid)/760 (liquid)
Specific heat [kJ/kg K]	2.9 (solid)/2.2 (liquid)
Thermal conductivity [W/m K]	0.2
Melting temperature [^{o}C]	47
Latent heat [kJ/kg]	140
Thermal expansion [K^{-1}]	0.001

A total of five T-type thermocouples are located at different locations shown in Fig. 3 for recording temperatures during phase change process. Thermocouples 1-5 are used for measuring the PCM temperature at different heights at different PCM partitions during melting. All exposed surfaces of the slab are fully insulated using glass wools which has a high thermal resistance of ~28^{o}C/W. The heater used is hot plate stirrer (model 209-1) from IEC Pty Ltd and the data acquisition unit used is Agilent 34970A for capturing the respective temperature at timely basis.

B. Physical model

A schematic 2-D computational domain for Fin type and Fin-Spiral fillers slab are shown in Fig. 3 and Fig. 5 respectively Due to geometrical symmetry of both rectangular

encapsulations, half of the geometry will be used in the modeling for time and memory saving during computation.

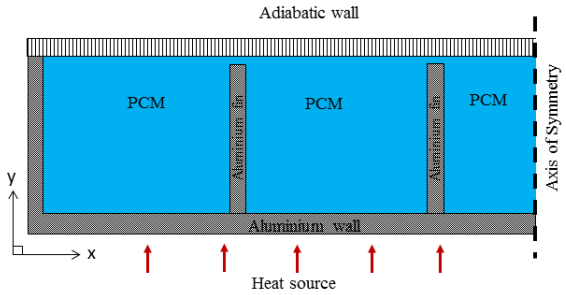

Fig. 3 Computational domain for fin type (4 fins) slab configuration.

In the experimental prototypes, thin air gap is designated in the ventilated slab environment to allow PCM expansion during heating. It is noted that air has very low thermal conductivity and thin air gap will eliminate natural convection heat transfer. Hence, modeling of air gap and PCM thermal expansion are neglected in this case.

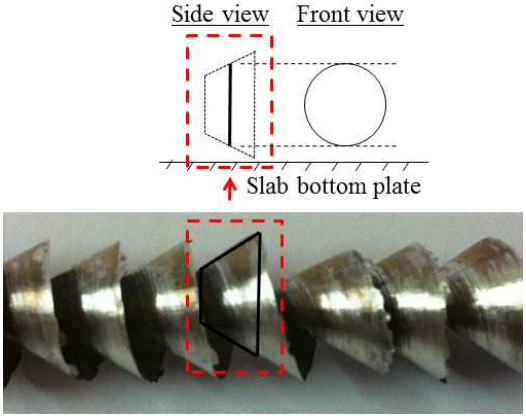

Fig. 4 Simplified computational model for spiral fillers

Fig. 4 shows an aluminum spiral filler strip used in the experiment. For two dimensional modeling, circular shape will be used to model aluminum circular wall for simplicity. The mean diameter of the helical shape will be used to represent the aluminum spiral filler walls in this two-dimensional numerical analysis. It is noted that there will be a PCM mass reduction using this simplified method under similar slab dimensions. A volume-corrected version has developed and validates with the experimental results.

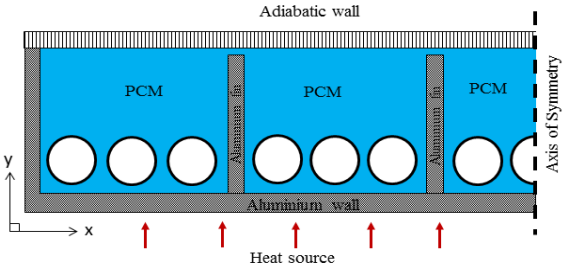

Fig. 5 Computational domain for Fin-Spiral fillers type slab configuration.

Boussinesq approximation was adopted to calculate the change in PCM density as a function of temperature in the liquid density given by:

$$\rho = \rho_o\left[1-\beta\left(T-T_m\right)\right] \tag{1}$$

and the relationship of buoyancy forces in the momentum equation is given by:

$$-\rho g = \rho_o g\left[\beta\left(T-T_m\right)-1\right] \tag{2}$$

where ρ_o is the reference density at melting temperature T_m and β is the thermal expansion which valued at 0.001 based on the data provided by Humphries and Griggs [9]. The dynamic viscosity of the liquid PCM is given by [10]:

$$\mu = 0.001\times\exp\left(-4.25+\frac{1790}{T}\right) \tag{3}$$

C. Governing equations

Enthalpy-porosity formulation [7] is adopted in solving phase change process of PCM. Similar set of governing equations used in the computation were referenced from Shatikan et al. [11] where he has simulated the PCM melting in rectangular Fin type partition storage. In this numerical study, volume of fluids (VOF) which used for simulating the two or more different fluids is not considered and volumetric expansion of PCM is negligible in this computational analysis.

Continuity:

$$\frac{\partial}{\partial x_i}\left(\rho u_i\right) = 0 \tag{4}$$

Momentum:

$$\frac{\partial}{\partial t}\left(\rho u_i\right)+\frac{\partial}{\partial x_i}\left(\rho u_i u_j\right) = \mu\frac{\partial^2 u_i}{\partial x_i x_j}-\frac{\partial P}{\partial x_i}+\rho g_i + S_i \tag{5}$$

Energy:

$$\frac{\partial}{\partial t}\left(\rho h\right)+\frac{\partial}{\partial x_i}\left(\rho u_i h\right) = \frac{\partial}{\partial x_i}\left(k\frac{\partial T}{\partial x_i}\right) \tag{6}$$

Where ρ is the density, k is the thermal conductivity, μ is the dynamic viscosity, S_i is the momentum source term, u_i is the

velocity component, x_i is the Cartesian coordinate and h is the specific enthalpy. The sensible enthalpy h_s is given by:

$$h_s = h_{ref} + \int_{T_{ref}}^{T} C_p dT \quad (7)$$

And the total enthalpy, H is defined as:

$$H = h_s + \Delta H \quad (8)$$

The total enthalpy is the sum of sensible enthalpy h_s and the enthalpy change due to phase change γL, where h_{ref} is the reference enthalpy at the reference temperature T_{ref} , C_p is the specific heat, L is the specific enthalpy of melting (liquid state) and γ is the liquid fraction during the phase change which occur over a range of temperatures $T_s < T < T_l$ defined by the following relations:

$$\gamma = \frac{\Delta H}{L} = 0 \quad \text{if} \quad T_s < T \quad [\text{Solid}] \quad (9)$$

$$\gamma = \frac{\Delta H}{L} = \frac{T - T_s}{T_l - T_s} \quad \text{if} \quad T_s < T < T_l \quad [\text{Mushy}] \quad (10)$$

$$\gamma = \frac{\Delta H}{L} = 1 \quad \text{if} \quad T > T_l \quad [\text{Liquid}] \quad (11)$$

The source term S_i in the momentum equation (eqn. 5) is given by:

$$S_i = -A(\gamma)u_i = \frac{C(1-\gamma)^2}{\gamma^3 + \varepsilon} u_i \quad (12)$$

Where $A(\gamma)$ is defined as the "porosity function" which governed the momentum equation mimic Carman-Kozeny equations for flow in porous media introduced by Brent et al. [12]. The function reduces the velocities gradually from a finite value as 1 in fully liquid to 0 in fully solid state within the computational cells involving phase change. The epsilon ε=0.001 infinity avoidance constant due to division by zero and C is a constant reflecting the morphology of the melting front where C = 10^5 was assumed in this study which had been used in by Shatikan et al. 11].

D.Computational Procedure

The SIMPLE algorithm is used for solving the mass, momentum and energy governing equations. Approximately about 150,000 triangular and quadrilateral cells are meshed for all configurations for solving the flow fields, melt fractions and temperature distributions. The time step selected is 0.1 second where comparative testing on time step of 0.01, 0.05 and 0.1 seconds had shown little difference which deemed to be neglected. Hence, larger time step of 0.1 second can be used for saving computational time. The maximum number of iteration for every time step was between 10 and 20 as recommended by Fluent [13].

III. Results and Discussion

In this section, melting visualizations have developed and discussed. As the experimental PCM slab prototypes are made of aluminum, melting process is not visible during testing. The developed melting front visualizations will be used as a predictive tool for observing the melting phenomenon.

A. Model validation

Model validation was performed by comparing of the numerically predicted temperature data with experimental data at thermocouple location (T2) showed in figure 3.

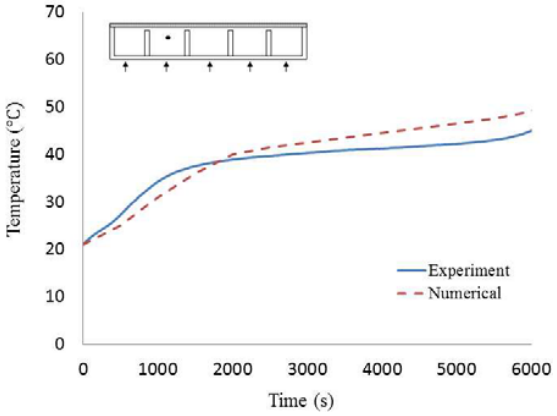

Fig. 6 Numerical and experimental results comparison for Fin type slab configuration at thermocouple T2

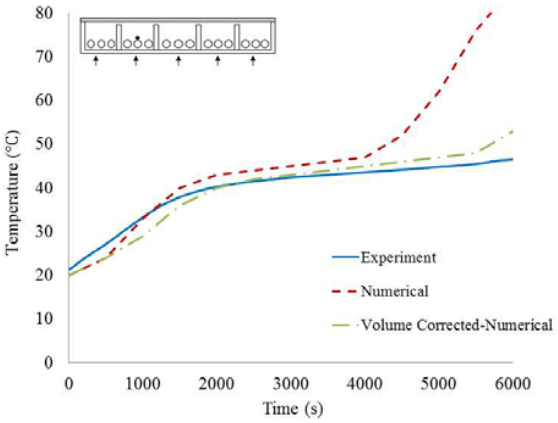

Fig. 7 Numerical and experimental results comparison for Fin-Spiral fillers slab configuration at thermocouple T2

Fig. 6 and 7 show the numerical and experimental temperature history comparison at the thermocouple location (T2). The validation shows good agreement between both data over time where both results stay within 4°C. It is also noted that the Fin-Spiral fillers slab configuration is modeled by using circular aluminum walls which will result lesser PCM volume as compared to Fin type configuration. As expected, the numerical model reaches fully liquid earlier, shorter phase change period and higher maximum temperature which is not

ideal for validation. However, the volume-corrected model which modified with the same amount of PCM filled has displayed a good agreement with the experimental results. Hence pre-volume corrected fin-spiral fillers will be used in the analysis.

B. Computational visualization

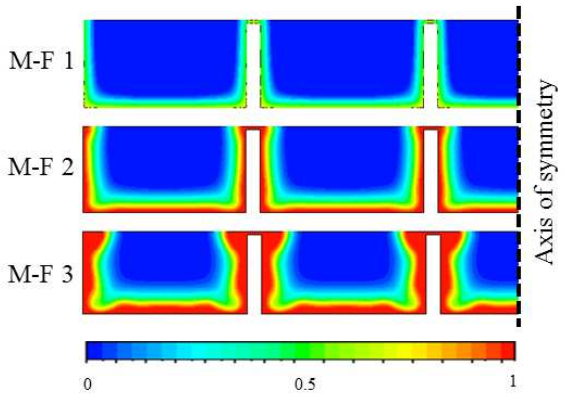

Fig. 8 Melt fraction for fin type (M-F 1/2/3) at 1800, 3600 and 5400 seconds respectively

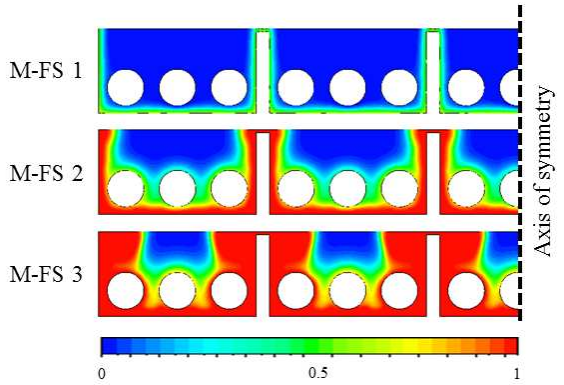

Fig. 9 Melt fraction for fin-spiral fillers (M-FS 1/2/3) at 1800, 3600 and 5400 seconds respectively

Fig. 8 and 9 present the melt fraction performance for Fin type and Fin-Spiral fillers type slab configurations under 1000W/m^2 of constant heating at the bottom part of the slab. Three different stages of melting: 1800 seconds (30 minutes), 3600 seconds (60 minutes) and 5400 seconds (90 minutes) are used in this analysis. It is clearly seen that both configurations have the similar melting performance at the first 30 minutes (M-F1 and M-FS1). Melting of PCM is initiated at the wall boundaries by heat conduction in the aluminum walls and fins. It is observed in the Fin-Spiral fillers slab configuration that melting front has formed around the aluminum wall surfaces and not at the aluminum spiral filler walls. This is due heat flow is hindered by the poor thermal conductivity of the PCM present in between. As heating continues, the melting behaviors of both configurations become very different in the later stages. At 60 minutes time stage, large portions of liquid fraction are seen forming around the aluminum spiral fillers in the Fin-Spiral fillers slab shows in Fig. 9 under M-FS2 melt fraction contour. The liquid fraction illustrated in red started to become wider and wavy as compared to Fin type slab as greater natural convection heat transfer has assisted in the melting process. Fin type slab (M-F2) shown in Fig. 9 has a steady melting pattern without any sign of abrupt change in melting front due to weaker natural convection effect. The natural convection effect is promoted by the PCM density difference which has an inverse function of increasing temperature in the liquid region. This will generate buoyancy forces which is able to dissipate heat to the other cooler regions of the PCM along the interface.

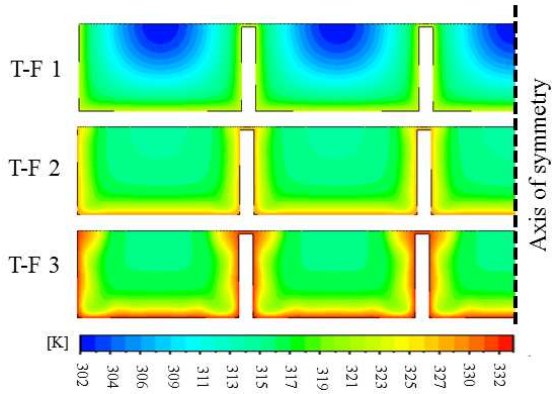

Fig. 10 Temperature distributions of fin type (T-F 1/2/3) at 1800, 3600 and 5400 seconds

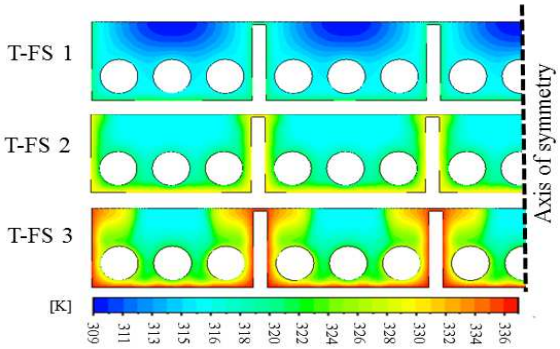

Fig. 11 Temperature distributions of fin-spiral fillers (T-FS 1/2/3) at 1800, 3600 and 5400 seconds

Fig. 10 and 11 show the temperature distributions for both slab configurations at different time stages. It is clearly seen that higher temperature range is present in Fin-Spiral filler slab compared to Fin type slab. This phenomenon shows that the natural convection current played a major role in reducing the thermal resistance of the LHS system.

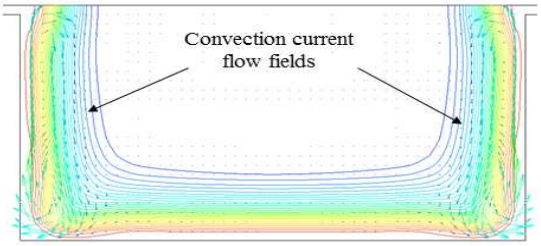

Fig. 12 Convective flow fields in 1 fin partition of Fin type configuration at 3600 seconds

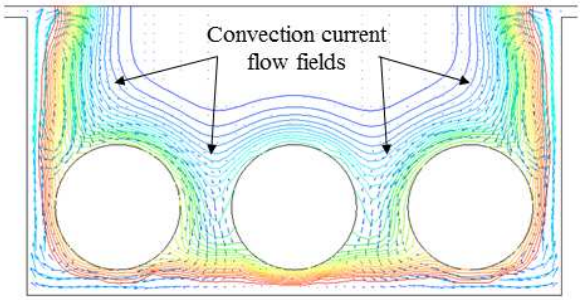

Fig. 3 Convective flow fields in 1 fin partition of fin-spiral filler configuration at 3600 seconds

Fig. 12 and 13 show the convective flow fields for both slab configurations at 60 minutes simulation. The convective flow fields represented in arrows and the contour lines represent the temperature boundaries of the melting PCM. In Fin type configuration, there is strong stream of vortices circulating near the fin walls, transfer heat from the hotter bottom region to the top cooler region. This convective heat transfer circulation assisted melting solid-liquid interface near the walls but it still maintained a high thermal resistance in the middle cooler region where heat was not effective penetrated. As for Fin-Spiral fillers configuration, adding aluminum spiral fillers to Fin type slab will reduce the convective heat transfer effect due to lower temperature gradients but improve melting at the middle region of the PCM through heat conduction. However, it is clearly seen that there are more regions of convective vortices present around the circular wall which will eventually grow stronger with greater liquid fraction formation. This is due to the higher thermal conductivity of aluminum spiral filler assisted in expanding more liquid regions at the middle section and resulted more temperature driven vortices for heat dissipation than Fin type configuration.

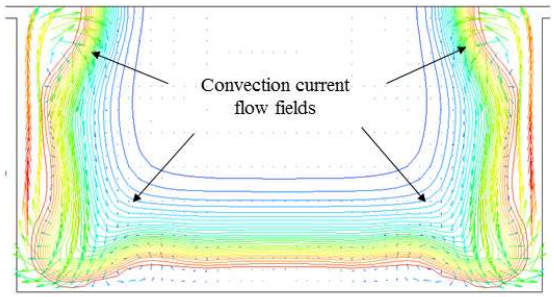

Fig. 4 Convective flow fields in 1 partition of Fin type configuration at 5400 seconds

Fig. 14 and 15 show the behaviors of natural convective currents at the latter stage of melting. There are multiple regions of active convective flow fields propagating in the Fin-Spiral fillers slab, especially at the aluminum spiral fillers regions. This active flow effect would reduce the thermal resistance of the mushy zone by dissipating heat to the cooler region in slab. As for Fin type slab, the convective flow fields seemed to be active around the heated wall region and weaker at the melting interface. Hence, the heat transfer will be less effective as it creates a thermal resistance for the heat to enter into the core of the solid PCM.

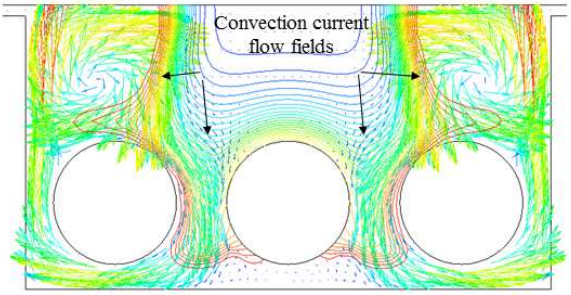

Fig. 5 Convective flow fields in 1 fin partition of fin-spiral filler configurations at 5400 seconds

It is noted that the dominance heat transfer in PCM is conduction in solid state and natural convection in liquid state. It is clearly seen that Fin-Spiral fillers configuration developed greater liquid fraction than fin type over the same period of time. A melt fraction for Fin type, Fin-spiral filler and volume-corrected fin-spiral fillers configurations are compared and shows in Fig. 16.

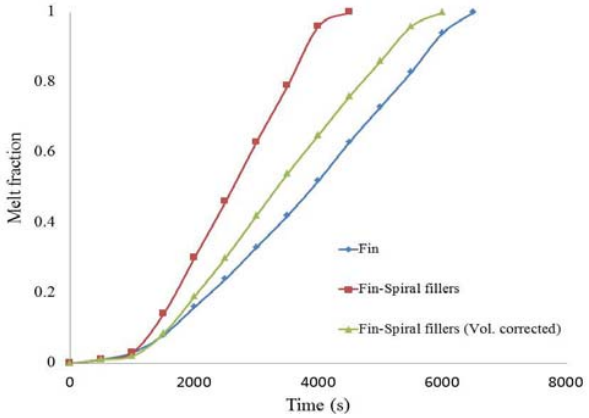

Fig. 6 Numerically predicted melt fraction comparison for Fin and Fin-Spiral fillers configurations.

The melt fraction representation evaluates the melting performance of PCM in different heat enhancement configurations with respect to time. Based on the results show in Fig. 16, by adding spiral fillers into PCM slab can improve melting rate. In comparison between Fin and Fin-Spiral fillers (Volume-corrected), the numerical results show that the addition of aluminum spiral fillers has a faster melting performance with the same amount of PCM filled.

IV. Conclusions

In this present work, melting performance in Fin and Fin-Spiral fillers configurations has been numerically investigated.The numerically analysis is conducted based on enthalpy-porosity formulation and the simulated results are validated with the experimental data.

The following conclusions are drawn:

- Adding aluminum spiral fillers into Fin type LHS will improves heat conduction but reduce natural convective effect at early stage of melting. However, melting rate speed up in the latter stage where spiral fillers promote more regions of natural convective currents at melting interfaces which will increase the melting rate.
- The visualization of Fin-Spiral fillers configurations have shown better melting performance than the Fin type configuration by promoting smaller but more natural convection currents at the middle region near the core of the solid PCM. This will assist melting as more heat is dissipated to the solid PCM through natural convection.
- This proposal of using aluminum spiral fillers as an alternative thermal enhancement method for LTS system. It is simple and effective where it does not require much manufacturing complexity than using close-gap fins approach.
- Further research on using smaller and more spiral fillers are recommended for higher melting rate as it is expected to increase the heat conduction and able to promote more natural convective regions within the PCM fin partitions.

Acknowledgment

The authors wish to thank Dr. Panniselvam from Department of Chemical Engineering RMIT University for his kind support in DSC scanning on samples of paraffin wax.

Nomenclature

ρ	Density
ρ_o	Reference density
β	Thermal expansion
T_m	Melting temperature
T_s	Solidus temperature
T_l	Liquidus temperature
g	Gravity
μ	Dynamic viscosity
S_i	Momentum source term
h	Specific enthalpy
k	Thermal conductivity
h_s	Sensible enthalpy
h_{ref}	Reference enthalpy
C_p	Specific heat
H	Total enthalpy
L	Latent heat
γ	Liquid fraction
ε	Infinity avoidance constant
C	Morphology melting constant

References

[1] Morisson, Abdel-Kalik, 1978. Effect of phase-change energy storage on the performance of air-based and liquid-based solar heating sytems. *Solar Energy* 20: 57-67.

[2] A.A. Ghoneim, 1989. Comparison of theoretical models of phase-change and sensible heat storage for air and water-based solar heating systems. *Solar Energy* 42(3): 209-20.

[3] A. G. Evans, M.Y. He, Hutchinson J.W., Shaw M., 2001. Temperature distribution in advanced power electronics systems nd the effect of phase change materials on temperature supprression during power pulses. *J. Electron. Packag.-Trans. ASME* 123: 211-217.

[4] S. Jegadheeswaram, S.D. Pohekar, 2009. Performance enhancedment in latent heat thermal storage system: A review. *Renewable and Sustainable Energy Reviews* 13: 2225-2244.

[5] S.M. Hasnain, 1998. Review on sustainable thermal storage technologies, Part 1: Heat storage materials and techniques. *Energy Convers Mgmt* 39: 1127-3-1138.

[6] M. Gharebagi, I. Sezai, 1997. Enhancement of heat transfer in latent heat storage modules with internal fins. *Numer Heat Transf* Part A 53: 749-765.

[7] P. Lamberg, K. Siren, 2004. Numerical and experimental investigation of melting and freezing processes in phase change material storage. *Int J. Therm Sci* 43: 277-287.

[8] Y. Jellouli, R. Chouikh, A. Guizani, A. Belghith, 2007. Numerical study of the moving boundary problem during melting process in a rectangular cavity heated from below. Am J. App Sci 4: 251-256.

[9] W.R. Humphries, E.I. Griggs, 1977. A design handbook for phase change thermal scontrol and energy storage devices. NASA Technicsal Paper 1074, NASA Scientific and Technical Information Office.

[10] R. Reid, J. Prausnitz, B. Poling, 1987. The Properties of Gases and Liquids, McGraw-Hill, New Yorok.

[11] V. Shatikan, G. Ziskind, R. Letan, Numerical investigation of a PCM-based heat sink with internal fins. *Int. J. Heat and Mass Transfe*r 48 (2005) 3689-3706.

[12] A.D. Brent, V.R. Voller, K.J. Reid, 1988. Enthalpy-porosity technique for modeling convection-diffusion phase change: Application to the melting of a pure metal, *Numer*. *Heat Transfer* 13: 297-318.

[13] ANSYS Inc., ANSYS Fluent 12.0 User's Guide, 2009